ELSEVIER

Non-radiative processes of excited CT states of Ru(II) and Pt(II) compounds and excited d–d states of Rh(III) compounds in the solid state and at higher temperatures

Ashraful Islam, Noriaki Ikeda, Koichi Nozaki, Yasuyuiki Okamoto,
Bovak Gholamkhass, Akio Yoshimura, Takeshi Ohno

*Department of Chemistry, Graduate School of Science, Osaka University,
1-16 Machikaneyama, Toyonaka, Osaka 560, Japan*

Contents

Abstract

Radiative and non-radiative processes of excited CT states of Ru(II) and Pt(II) compounds and excited d–d states of Rh(III) compounds in the solid state and at higher temperatures are examined. A rapid non-radiative transition of a metal-to-ligand charge transfer excited state to the ground state does not occur over a wide temperature range (77–300 K) for [Ru(bpy)$_3$](PF$_6$)$_2$ and [Pt$_2$(tpy)$_2$(guanidinato)](ClO$_4$)$_3$. Spectral simulations of the d–d emissions of Rh(III) compounds in the range 77–536 K are carried out by assuming a simple configuration coordinate. The large Huang–Rhys factors indicate that the lowest and second lowest d–d excited states of Rh(III) compounds are strongly coupled to the excited vibrational state of the ground state. The frequency factors of non-radiative decay are 10^{11}–10^{12} s^{-1} for the excited triplet state. © 1998 Elsevier Science S.A.

Keywords: Nonradiative processes; CT excited states; d–d Excited states; Ru(II); Pt(II); Rh(III)

1. Introduction

Most chemical reactions occur as a transition between the electronic states accompanied by a change of the nuclear configuration. The rates of the chemical reaction are, therefore, governed not only by the energy matrix element, but also by the Franck–Condon weighted density. An excited molecule in a bimolecular electron transfer (ET) process, for instance, is non-radiatively converted to a redox product with a displaced nuclear configuration with respect to the excited molecule. If a large inner sphere reorganization energy is involved in the ET, the rate of ET in a Marcus inverted region does not decrease rapidly as the exergonicity increases. This comes from the large Franck–Condon factor for the transition between the ground vibrational state of the initial excited state and the excited vibrational states of the product.

Van Houten and Watts [1,2], 20 years ago, found a fast non-radiative transition of the excited $[Ru(bpy)_3]^{2+}$ in solution at higher temperatures. Meyer and coworkers [3], Barigelletti et al. [4] and Balzani and coworkers [5] made elaborate studies on the endergonic non-radiative transition of excited MLCT state in solution and gave a well-known explanation that the thermal excitation of MLCT triplet excited state to a considerably displaced d–d triplet excited state is followed by the efficient intersystem crossing to the ground state. One of the outcomes is that the frequency factor of the internal conversion from ^{3}MLCT to the displaced ^{3}(d–d) is close to the largest possible value of 10^{14} s^{-1}.

However, there seems to be no direct evidence for not only the formation of ^{3}(d–d) from ^{3}MLCT, but also the displaced nuclear configuration of the excited triplet d–d state of a Ru(II) compound. Therefore, we have investigated non-radiative processes of two kinds of excited states, MLCT excited states of Ru(II) and Pt(II) compounds and d–d excited states of Rh(III) compounds, in the solid state and over a wide temperature range. In order to look at the nuclear configuration of the excited states, emission spectra have been examined.

2. Results and discussion

2.1. Non-radiative decay of MLCT states of $[Ru(bpy)_3](PF_6)_2$ [6] and $[Ru(tpy)_2](ClO_4)_2$ [7] at higher temperatures

The ^{3}CT state of a crystalline sample of $[Ru(bpy)_3](PF_6)_2$ at room temperature emits a structured phosphorescence whose peak is invariant with temperature below 300 K. This temperature-independence of the peak energy in the solid state is in contrast to a large low energy shift in fluid solution [8]. The decay rate of emission is almost independent of temperature (2–5 μs) for the solid sample in the temperature range 77–350 K. A rapid increase of the non-radiative decay rate of the ^{3}MLCT occurred suddenly above 350 K. The Arrhenius plot of the decay rate constant shows that the activation energy of the non-radiative decay of the ^{3}MLCT is so high (5000 cm^{-1}) that the rate-determining step of the non-radiative decay for

$[Ru(bpy)_3](PF_6)_2$ is the endergonic internal conversion to $^3(d–d)$. The large frequency factor $(7 \times 10^{13}\ s^{-1})$ of the internal conversion indicates that the nuclear displacement of the lowest triplet d–d state with respect to the ^3MLCT state is so large that the internal conversion occurs as an adiabatic process as depicted in Fig. 1.

As for $[Ru(tpy)_2](ClO_4)_2$, McMillin and coworkers [9] speculated that the energy level of $^3(d–d)$ lies close to ^3CT. The basis for their speculation is that the nitrogen atoms of terminal pyridines of 2,2′:6′,2″-terpyridine are distant so that the ligand field strength on the $Ru(II)$ ion is weaker than that in $[Ru(bpy)_3]^{2+}$. Actually, the activation energy of the non-radiative decay was low $(1100–2000\ cm^{-1})$. Since the weakly endergonic internal conversion to $^3(d–d)$ is thought to be very rapid, the intersystem crossing of $^3(d–d)$ to the ground state could be the rate-determining step of ^3MLCT decay. The frequency factors obtained from the Arrhenius plot of the decay rate are $10^{11}–10^{12}\ s^{-1}$, which are much smaller than those of the endergonic internal conversion of $[Ru(bpy)_3](PF_6)_2$. The small frequency factor of the intersystem crossing can be related to either the small energy matrix element or the small Franck–Condon weighted density. Since, however, no emission is observed from the excited d–d state of $Ru(II)$ compounds, no quantitative argument can be made regarding the intersystem crossing.

2.2. Non-radiative decay of MLCT state of $[Pt_2(tpy)_2(guanidinato)](ClO_4)_3$ [10]

Che and coworkers [11] reported that the title compound contained a 3.07 Å long bond between $Pt(II)$ ions and the planes of 2,2′:6′,2″-terpyridine are kept parallel. The solid sample at 77 K exhibits an emission spectrum with the maximum at 14 400 cm^{-1} and a FWHM of 1900 cm^{-1} as shown in Fig. 2. On raising the temperature to 300 K, the band became broader and the peak shifted to higher energy, as seen for $[Pt_2(H_2P_2O_5)_4]^{4-}$ [12]. The decay rate of the emission of crystalline samples is dependent on temperature over a wide temperature range. A formal analysis of the Arrhenius plot gives rise to a small frequency factor $(1.3 \times 10^8\ s^{-1})$ for the crystal sample, which implies that the nuclear configuration of MLCT itself is poorly
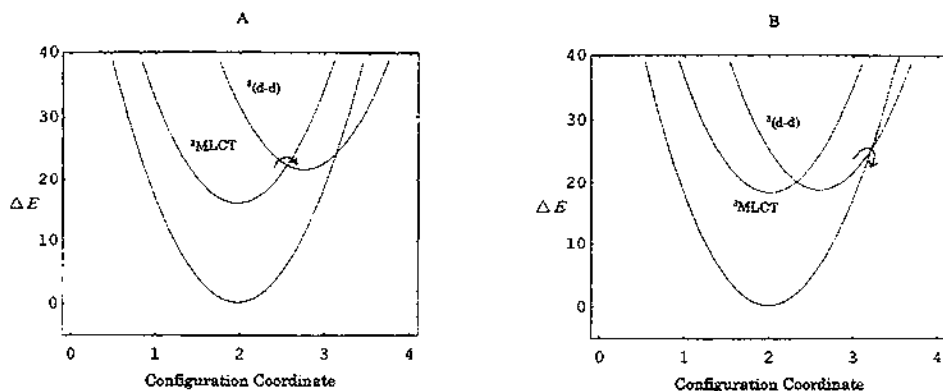

Fig. 1. Schematic potential diagram of ^3MLCT and $^3(d–d)$ along a single configuration coordinate. Arrows show either internal conversion or intersystem crossing. (A) $[Ru(bpy)_3](PF_6)_2$; (B) $[Ru(tpy)_2](PF_6)_2$.
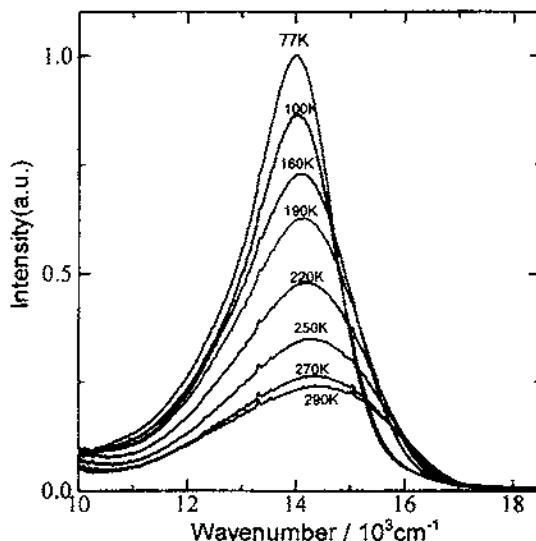
Fig. 2. Temperature-dependent decay of emission of [Pt₂(tpy)₂(guanidinato)](ClO₄)₃ in the solid state.

displaced in comparison with the Rh(III) compounds (vide infra). The excited state absorption of the compound adsorbed on SiO_2 exhibits a broad band below $20\ 000\ cm^{-1}$ and a strong band at $27\ 000\ cm^{-1}$ (Fig. 3). Since the absorption peak at $27\ 000\ cm^{-1}$ was seen for the excited Ru-to-tpy CT state [13], the assignment of the emission as Pt(II) chromophore-to-tpy CT [11,14] is supported.

The binuclear Pt(II) compound in ethanol–DMF at 77 K exhibits a CT emission at a slightly lower energy than the crystal does; and with quantum yield at 77 K high (0.41) in comparison with that of $[Ru(bpy)_3]^{2+}$. While the band peak at 77 K is a little lower in energy than it is in acetonitrile at 300 K, the agreement of the emission–excitation with the absorption spectrum for the sample in ethanol–DMF at 77 K (Fig. 4) indicated that the emission originates from the title compound. The emission quantum yield, however, was very much reduced above the melting point of the mixed solvent. The much shorter lifetime of the excited state in fluid solvent was determined by means of picosecond laser kinetic spectroscopy. The lifetime of MLCT excited state was 28 ps at ambient temperature. The Arrhenius plot of the decay rate of the excited state absorption gives rise to the large frequency factor $(2 \times 10^{12}\ s^{-1})$ of the solution sample as is shown in Fig. 5. It demonstrates that the non-radiative transition of the MLCT state in solution may be strongly perturbed by solvent molecules at the axial positions of the double planar binuclear Pt(II) compound. Solvent effects on the d-orbitals of the Pt(II) chromophore may play an important role in the non-radiative decay of the MLCT state.

2.3. Non-radiative decay of cis-[Rh(bpy)₂Cl₂](PF₆) at higher temperatures [15]

The lowest excited state, ^{3}(d–d), of [Rh(bpy)₂Cl₂](PF₆) exhibits as broad an emission as those of other Rh(III) complexes studied at 77 K [16,17]. The temper-

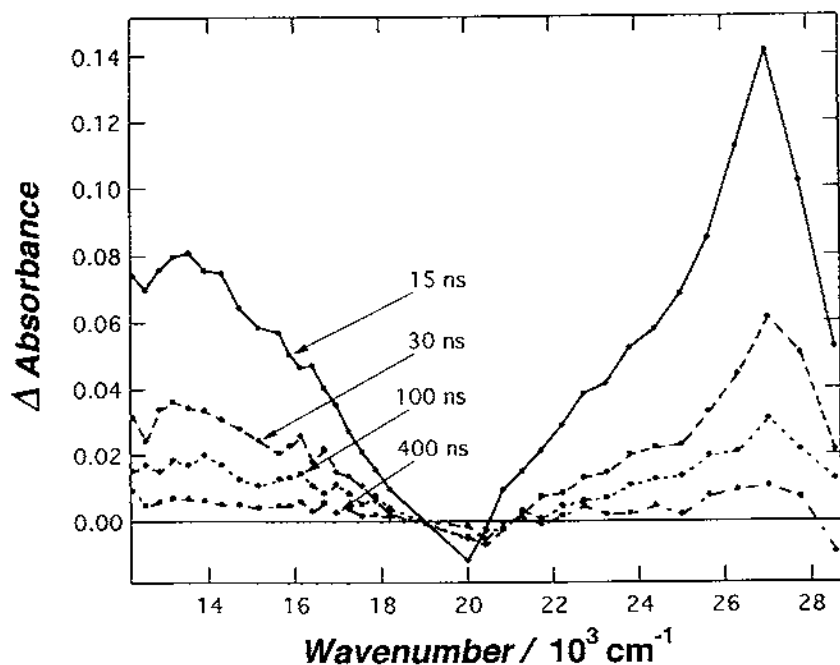Fig. 3. Excited-state absorption of [Pt₂(tpy)₂(guanidinato)](ClO₄)₃ adsorbed on SiO₂ at 298 K.
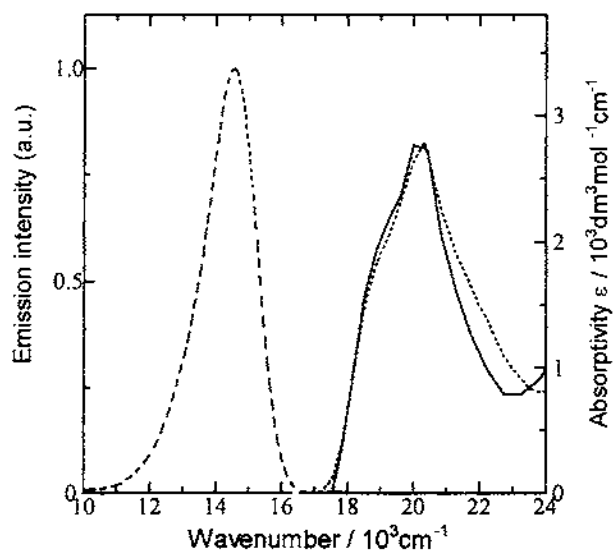
Fig. 4. Absorption, emission and emission-excitation spectra of [Pt₂(tby)₂(guanidinato)](ClO₄)₃ in 10:1 ethanol: DMF mixed solvent at 77 K. Solid line: absorption spectrum, dotted line: emission excitation spectrum and broken line: emission spectrum on the excitation at 20500 cm⁻¹.
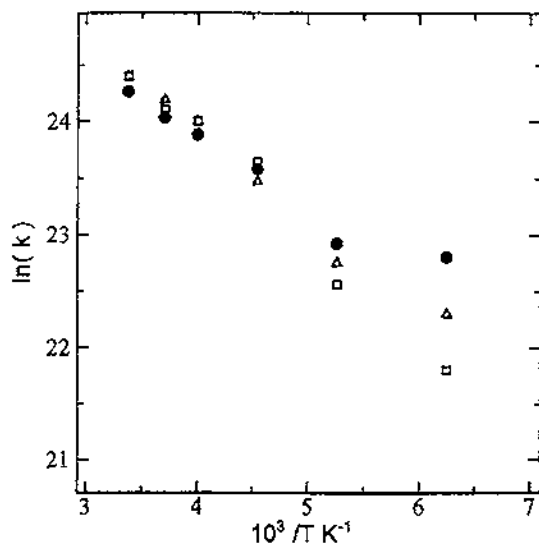
Fig. 5. Temperature-dependent decay of the excited-state absorption of [Pt$_2$(tpy)$_2$(guanidinato)](ClO$_4$)$_3$ in 10:1 ethanol:DMF mixed solvent. ● 730 nm, △ 600 nm, ▢ 420 nm.

ature dependence of the emission spectrum is unusual: the peak energy of the emission shifts significantly with temperature from 14 600 cm^{-1} at 77 K to 13 200 cm^{-1} at 536 K, and the FWHM of the emission increased from 2850 cm^{-1} at 77 K to 5450 cm^{-1} at 536 K. The unusual temperature effect on the emission spectrum can be interpreted in terms of a two-emitting-state model shown in Fig. 6. The higher temperature emission is decomposed into two emissions, one with a maximum at 14 600 cm^{-1} coming from the lowest d–d state [^{3}(d–d)$_1$, E], and the other with a maximum at 12 800 cm^{-1} from the second lowest d–d state [^{3}(d–d)$_2$, A$_2$]. A spectral simulation was made using a vibrational frequency of 400 cm^{-1} and two Huang–Rhys factors and assuming no population of the high vibrational excited level. The Huang–Rhys factors of the high energy and the low energy emissions are 11 and 16, respectively. The low energy emission of the second lowest ^{3}(d–d) states lying higher by 150 cm^{-1} has a larger Franck–Condon energy (6400 cm^{-1}) than that (3700 cm^{-1}) of the high energy emission. The larger Huang–Rhys factor or the larger Franck–Condon energy implies the second lowest d–d state is more displaced with respect to the ground state.

The thermal excitation of ^{3}(d–d)$_1$ (E) to ^{3}(d–d)$_2$ (A$_2$) is supported by an Arrhenius plot of the decay rate. The activation energy of the decay process in a temperature range of 160–400 K corresponds to the energy of the barrier crossing between ^{3}(d–d)$_1$ and ^{3}(d–d)$_2$. The thermal activation of the decay in a range of 400–536 K is the exergonic non-radiative intersystem crossing from ^{3}(d–d)$_2$ to the ground state. The most interesting thing is that the frequency factor of non-radiative intersystem crossing (7×10^{11} s^{-1}) is close to that found for [Ru(tpy)$_2$](ClO$_4$)$_2$. The inefficient intersystem crossing of ^{3}(d–d)$_2$ can be rationalized as a formally spin-forbidden
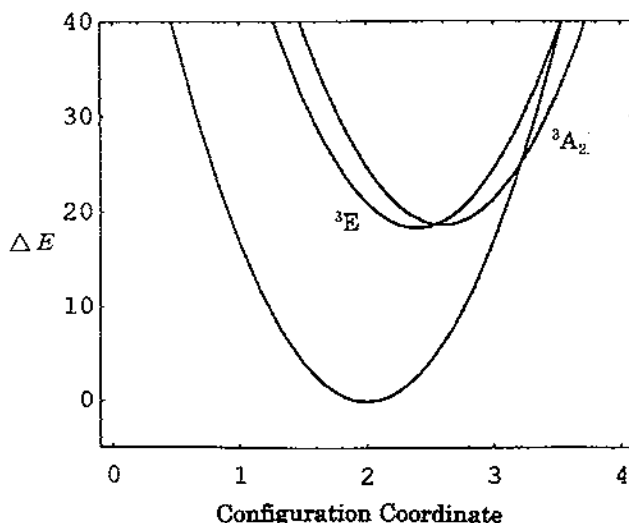
Fig. 6. Schematic potential diagram of $^3(d-d)_1$ (^3E) and $^3(d-d)_2$ ($^3A_2$) along a single configuration coordinate for $[Rh(bpy)_2Cl_2](PF_6)$.

process. An alternative explanation for the low frequency factor is based on the nuclear tunneling between the second lowest d–d state and the ground state. If the nuclear tunneling occurs from the excited electronic states to the excited vibrational states of the ground electronic state, the intersystem crossing rate is not so slow at lower temperatures. The contribution of nuclear tunneling to the intersystem crossing lowers the slope and the intercept of the Arrhenius plot.

2.4. Non-radiative decay of trans-[Rh(en)$_2$Cl$_2$](PF$_6$) at higher temperatures [18]

For the sake of simple simulation of the emission spectrum, both the *trans*- and the *cis*-forms of [Rh(en)$_2$Cl$_2$](PF$_6$) have been examined. The optical absorption spectra reveal [19] that the second lowest excited d–d state, $^3A_2$, of *trans*-[Rh(en)$_2$Cl$_2$](PF$_6$) lies too high to be thermally excited from the lowest one, ^3E. A very small high-energy shift of the emission peak with temperature indicates only an emission from the lowest d–d excited state (^3E) of *trans*-[Rh(en)$_2$Cl$_2$](PF$_6$) as is shown in Fig. 7, while the emission of the *cis*-form exhibited a peak shift of $200\,cm^{-1}$ to low energy because of the mixing of two emissions from $^3A_2$ and ^3E. Furthermore, the emission of *trans*-[Rh(en)$_2$Cl$_2$](PF$_6$) at 77 K exhibits weak vibronic bands with a spacing of $250\,cm^{-1}$. The emission spectrum of the *trans*-form over a wide temperature range (77–460 K) was simulated by using two parameters: a vibrational frequency of $250\,cm^{-1}$ and a Huang–Rhys factor of 20. The Franck–Condon factor of nuclear tunneling between the mth excited vibrational state of ^3E and the nth excited vibrational state of the ground state is evaluated by using the following equation. The large number of the Huang–Rhys factor implies
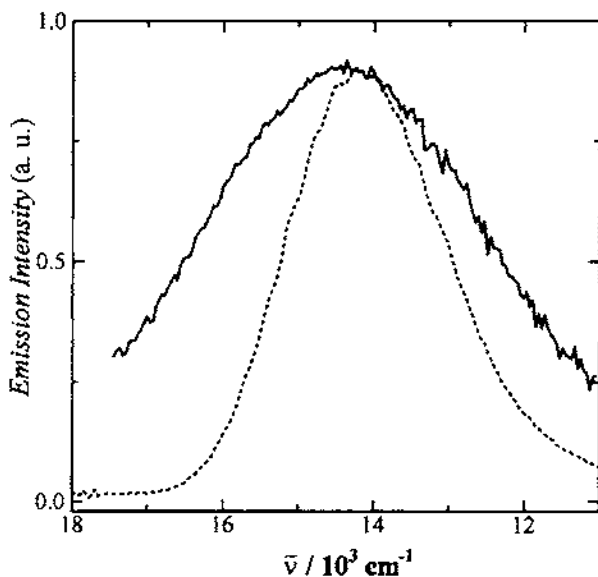
Fig. 7. Emission spectra of trans-[Rh(en)₂Cl₂](PF₆). Solid line 468 K, dotted line 77 K.

that the displacement of the ^3E state is very large.

$$\langle n|m\rangle = \sqrt{n!m!}\; S^{(n-m)/2} \sum_{j=0}^{m} (-1)^j \frac{S^j \exp\left(-\dfrac{S}{2}\right)}{(m-j)!j!(n-m+j)!} \qquad (1)$$

The decay rate of emission is independent of temperature below 250 K and strongly dependent on temperature above 250 K. The frequency factor obtained from the Arrhenius plot of the decay rate in the higher temperature region is small ($10^{10}\,s^{-1}$ for the cis-form and $10^{12}\,s^{-1}$ for the trans-form) compared with the exergonic internal conversion of $[Ru(bpy)_3](PF_6)_2$ between ^3MLCT and $^3(d-d)$. The rates of non-radiative transition via tunneling are estimated by using the parameters obtained from the spectral simulation. The temperature-dependent rates above 250 K can be obtained by taking the low frequency mode of vibration into consideration. The temperature-independent decay can never be explained using the parameter set. In order to represent the temperature-dependent rate over the whole temperature range, the participation of another vibrational mode of a high frequency vibration and a moderate Huang–Rhys factor must be taken into account. If this is the case, the magnitude of Huang–Rhys factor of the low frequency mode could be lower than 21. After all, it is incorrect to interpret the temperature dependence of the decay rate based on the two spectral parameters, the vibration frequency and the Huang–Rhys factor. Not only a more accurate spectral simulation of the emission at 4 K, but also the isotope effect on the emission decay should be examined.

3. Conclusion

Broad emission spectra of cis-[Rh(bpy)$_2$Cl$_2$](PF$_6$) at higher temperatures are decomposed into two emissions: one emission with the peak at $14\,600\,\text{cm}^{-1}$ comes from the lowest excited state and the other with the peak at $12\,800\,\text{cm}^{-1}$ from the second lowest d–d state. The Franck–Condon energy of the emission from the second lowest d–d state is as high as $6400\,\text{cm}^{-1}$. The emission spectra of trans-[Rh(en)$_2$Cl$_2$](PF$_6$) in a wide temperature range of 77–460 K are simulated by using a large Huang–Rhys factor (20) and frequency of vibration ($250\,\text{cm}^{-1}$). Meanwhile, the temperature dependence of non-radiative decays of excited trans-[Rh(en)$_2$Cl$_2$](PF$_6$) is not interpreted in terms of a simple configuration coordinate. The frequency factors of the non-radiative decay processes are 10^{10}–$10^{12}\,\text{s}^{-1}$ for the displaced excited d–d state of the Rh(III) compounds studied here.

The large frequency factor of the non-radiative transition of ^{3}MLCT of [Ru(bpy)$_3$](PF$_6$)$_2$ is ascribed to the endergonic internal conversion to a high lying d–d excited state, while the small frequency factor for the decay of ^{3}MLCT state of [Pt$_2$(tpy)$_2$(guanidinato)](ClO$_4$)$_3$ implies a poorly displaced configuration of ^{3}MLCT.

References

[1] J. Van Houten, R. Watts, J. Am. Chem. Soc. 97 (1975) 3843.
[2] J. Van Houten, R. Watts, Inorg. Chem. 17 (1978) 3381.
[3] B. Durham, J.V. Casper, J.K. Nagle, T.J. Meyer, J. Am. Chem. Soc. 104 (1982) 4803.
[4] F. Barigelletti, P. Belser, A. von Zelewsky, V. Balzani, J. Phys. Chem. 89 (1985) 3680.
[5] M. Maestri, N. Armaroli, V. Balzani, E.C. Constable, T. Cargill, Inorg. Chem. 34 (1995) 2759.
[6] A. Islam, N. Ikeda, K. Nozaki, T. Ohno, Chem. Phys. Lett. 363 (1996) 209.
[7] A. Islam, N. Ikeda, T. Ohno, Inorg. Chem., in press.
[8] N. Kitamura, H.-B. Kim, Y. Kawanishi, R. Obata, S. Tazuke, J. Phys. Chem. 90 (1986) 1468.
[9] C.R. Hecker, K.I. Grushurst, D.R. McMillin, Inorg. Chem. 30 (1991) 538.
[10] Y. Okamoto, N. Ikeda, B. Gholamkhass, A. Yoshimura, T. Ohno, in preparation.
[11] H.-K. Yip, C.-M. Che, Z.-Y. Zhou, T.C.W. Mak, J. Chem. Soc., Chem. Commun. (1992) 1369.
[12] J.A. Bailey, V.M. Miskowski, H. Gray, Inorg. Chem. 232 (1993) 369.
[13] J.R. Winkler, T.L. Netzel, C. Creutz, N. Sutin, J. Am. Chem. Soc. 109 (1987) 2381.
[14] A. Islam, N. Ikeda, K. Nozaki, T. Ohno, J. Photochem. Photobiol. A 106 (1997) 61.
[15] A. Islam, N. Ikeda, K. Nozaki, T. Ohno, XII ISPPCC Abstract, 1997.
[16] D.H.W. Carstens, G.A. Crosby, J. Mol. Spectrosc. 34 (1970) 113.
[17] T.R. Thomas, R.J. Watts, G.A. Crosby, J. Chem. Phys. 59 (1973) 2123.
[18] W.H. Fonger, C.W. Struck, J. Chem. Phys. 60 (1974) 1994.
[19] S.A. Johnson, F. Basolo, Inorg. Chem. 1 (1962) 925.